Euro. Jnl of Applied Mathematics (2000), *vol.* 11, *pp.* 433–452. Printed in the United Kingdom

Fluvio-deltaic sedimentation: A generalized Stefan problem

J. B. SWENSON[1,2,4], V. R. VOLLER[1,3], C. PAOLA[1,2], G. PARKER[1,3] and J. G. MARR[1]

[1] *Saint Anthony Falls Laboratory, University of Minnesota, Minneapolis, MN 55414*
[2] *Department of Geology and Geophysics, University of Minnesota, Minneapolis, MN 55455*
[3] *Department of Civil Engineering, University of Minnesota, Minneapolis, MN 55455*
[4] *Department of Geological Sciences, University of Minnesota, Duluth, MN 55812*

(*Received 1 September 1999; revised 15 March 2000*)

We present a model of sedimentation in a subsiding fluvio-deltaic basin with steady sediment supply and unsteady base level. We demonstrate that mass transfer in a fluvio-deltaic basin is analogous to heat transfer in a generalized Stefan problem, where the basin's shoreline represents the phase front. We obtain a numerical solution to the governing equations for sediment transport and deposition in this system via an extension of a deforming-grid technique from the phase-change literature. Through modification of the heat-balance integral method, we also develop a semi-analytical solution, which agrees well with the numerical solution. We construct a space of dimensionless groups for the basin and perform a systematic exploration of this space to illustrate the influence of each group on the shoreline trajectory. Our model results suggest that all subsiding fluvio-deltaic basins exhibit a standard autoretreat shoreline trajectory in which a brief period of shoreline advance is followed by an extended period of shoreline retreat. Base-level cycling produces a shoreline response that varies relative to the autoretreat signal. Contrary to previous studies, we fail to observe either a strong phase shift between shoreline and base level or a pronounced attenuation of the amplitude of shoreline response as the frequency of base-level cycling decreases. However, the amplitude of shoreline response to base-level cycling is a function of the basin's age.

1 Introduction

A sedimentary basin is a significant thickness of genetically related sedimentary rock that accumulates due to subsidence of the earth's crust over geologic time scales [1]. The creation and destruction of sedimentary basins are attributable to the movement of rigid lithospheric plates that comprise the earth's upper mantle and crust; sedimentary basins are thus a direct consequence of plate tectonics. Tectonic uplift of the earth's crust exposes previously buried rocks, including ancient sedimentary basins, to the surficial processes of erosion and long distance transport by rivers, which together create a supply of sediment and deliver it to regions of tectonically driven crustal subsidence, where it accumulates and is preserved as the deposits of a sedimentary basin. Subsidence is a necessary condition for the formation of a sedimentary basin; it is the only mechanism by which a significant thickness (kilometers) of sedimentary rock can accumulate. Regions of crustal uplift and net erosion commonly are separated from regions of subsidence and net

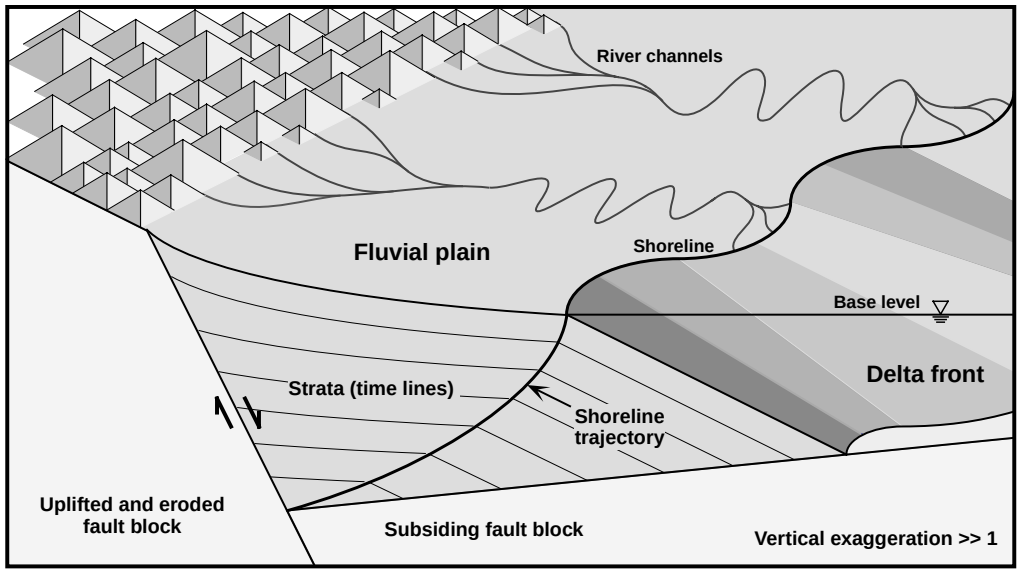

FIGURE 1. A simplified fluvio-deltaic basin.

sediment accumulation by fault zones in which tectonic stresses are dissipated via relative motion of the crust.

A fluvio-deltaic sedimentary basin consists of a subaerial fluvial plain, where sediment is transported and deposited by rivers, coupled to a subaqueous delta, where sediment transport and deposition occur via slope failure (avalanching), the settling of fine-grained sediments from suspension in the water column, and the entrainment and deposition of sediment by wind- and tide-generated currents. The boundary between the fluvial and deltaic regimes is the shoreline, where, by definition, the elevation of the earth's surface coincides with base level. For most basins, base level is sea level. Figure 1 shows a simplified fluvio-deltaic basin in which a long, linear fault zone separates a subsiding crustal block, which serves as a locus of sediment accumulation, from an uplifted and eroded crustal block, which is the basin's sediment source. To first order, the geometry of the basin is independent of the transverse (fault-parallel) direction. This independence is a consequence of the continual transverse migration and periodic reorganization of individual river channels on the fluvial plain, which, on geologic time scales, distribute sediment uniformly in the transverse direction. Because the river channels are the ultimate source of sediment for the delta, the same channel migration and switching are responsible for the uniform distribution of sediment across the width of the delta. The effects of currents enhance this transverse smearing process.

Preservation of depositional and erosional surfaces within the basin generates the strata that give sedimentary rocks a characteristic layered appearance at a variety of length scales. Stratigraphy is the study of the geometry and chronology of strata. In fluvio-deltaic basins the generation of large-scale stratigraphic signals is driven by three basin boundary conditions: (1) sediment supply to the basin, (2) the spatial distribution and rate of tectonic subsidence, and (3) base level. The stratigraphic evolution of a fluvio-deltaic basin can be envisioned as a competition between these boundary conditions.

Growth of the fluvial plain and delta is driven by the supply of sediment to the basin and the efficacy of its transport and deposition. Together these produce an increase in the elevation of the depositional surface and an overall lengthening of the fluvio-deltaic system. This lengthening is attenuated by tectonic subsidence, which lowers the depositional surface and creates space that must be filled for continued growth. The simplistic depositional strata (dashed lines) of Figure 1 reflect the evolution of this balance between sediment supply and subsidence. Fluctuations in base level can affect profoundly this balance by influencing the partitioning of sediment between the fluvial plain and the delta, which in turn determines the growth rate of one section relative to the other. A basin's strata record the complex superposition of these boundary conditions over its lifespan.

Stratigraphers use this record to solve the inverse problem: the strata are used to infer a basin's history of sediment supply, tectonism, and base level. Not unexpectedly, a unique solution to the inverse problem is difficult to obtain. A fundamental problem is the uncertainty and/or inapplicability of rock dating methods. Also, the identification and correlation of stratigraphic indicators are non-trivial and fraught with uncertainty. When observed at the outcrop scale, basin-scale stratigraphic indicators are commonly subtle features, often difficult to discern, and thus subject to the bias of human interpretation. Mapping of these features requires that they be correlated between outcrops, and the certainty of such correlation depends strongly on the frequency of outcrops, which in many locations is limited. Furthermore, crustal deformation associated with tectonic uplift and exposure of ancient basins often disrupts the lateral continuity of stratigraphic indicators and renders their correlation problematic.

In a fluvio-deltaic basin, the shoreline is associated with a relatively unambiguous lateral transition in grain size, sedimentary structures, and depositional slope that records the change from fluvial to submarine transport processes. The width of this transition zone, which is controlled by the strength of waves and tides and by the sediment grain size delivered to the delta, scales the uncertainty associated with the identification of shoreline in the basin's strata. In general, this width is small relative to the basin's characteristic length scale. Hence, in contrast to many basin-scale stratigraphic indicators, the ancient shoreline often can be identified with near certainty and its position tightly constrained.

The shoreline can be envisioned as an internal moving boundary of the fluvio-deltaic system. At any time, its lateral position is determined by a complex interaction of the basin's boundary conditions. Its trajectory preserved in the basin's strata provides a record of this interaction. An understanding of the shoreline response to sediment supply, tectonic subsidence, and base level is therefore of fundamental importance to stratigraphers interested in solving the aforementioned inverse problem. In addition, because the shoreline trajectory of many basins preserves information of past sea level, a careful comparison of shoreline trajectories from basins of similar age allows stratigraphers to reconstruct the history of global sea level.

Our objectives in this paper are to (1) develop a mathematical model of fluvio-deltaic sedimentation in a subsiding basin with fluctuating base level, (2) demonstrate that this model is a generalized Stefan problem, in which the shoreline represents the moving boundary, (3) identify a set of dimensionless groups associated with the problem, and (4) illustrate how these groups control the shoreline trajectory.

2 A basin filling model

2.1 Previous work

Previous models of basin-scale sedimentation on geologic time scales can be classified broadly as either geometric, in which some aspect (typically the slope) of the sediment-water interface is specified, or dynamic, in which the sediment-water interface evolves according to a quantitative representation of sediment transport and deposition. Pitman [16] presented a simple and elegant model, amenable to analytical solution, with which he studied the shoreline response to the rate of base-level fall. Angevine [2] extended Pitman's model to treat periodic fluctuations in the rate of base-level fall and demonstrated the existence of a frequency-dependent phase shift between shoreline position and base level. In addition, Angevine [2] showed that the amplitude of shoreline response to base level is strongly attenuated such that a basin behaves as a high-pass filter to base-level cycling. Jervey [7] and Posamentier and Vail [17] generated a suite of graphical, mass-conserving models in which the geometry of the fluvial plain and delta are known *a priori*.

Existing dynamic models of basin-scale sedimentation have focused generally on the generation and interpretation of strata and not on the determination of the shoreline trajectory. Kenyon and Turcotte [10] presented a diffusional model of equilibrium deltaic sedimentation in a non-subsiding, flat-bottomed basin in which *a priori* knowledge of the rate of shoreline advance was assumed. Paola *et al.* [14] addressed sedimentation in a purely fluvial basin, i.e. a basin without a submarine component, as a diffusional process with a moving boundary at the downstream terminus of the river network. Flemings & Jordan [4] and Jordan & Flemings [8] presented coupled, diffusional treatments of fluvial and submarine sedimentation in which the fluvial and submarine regimes were assigned different diffusivities. These authors did not discuss the moving-boundary aspects of their problems and, on the basis of computed shoreline position, enforced *a posteriori* conditions on the spatial distribution of diffusivity. Finally, Kaufman *et al.* [9] modeled fluvial and deltaic sedimentation as a non-linear diffusional process with a depth-dependent diffusivity.

2.2 Mathematical model

Consider a cross section through an idealized fluvio-deltaic basin such as that shown in Figure 2. A steady flux of sediment is delivered to the basin, $0 \leqslant x \leqslant L$, as a line source of strength q_{so} at $x = 0$. The basement of the basin, $b(x,t)$, is subsiding under the influence of regional tectonism at a specified, steady, and spatially variable rate, $\sigma(x)$, where σ is measured positive downward and has a mean value $\overline{\sigma}$. The base level, $Z_{bl}(t)$, can vary in time in a prescribed manner with an amplitude and period of A and T, respectively. We denote by $s(t)$ and $u(t)$, respectively, the positions of the shoreline and the intersection of the delta toe with basement. The elevation of the sediment-water interface is $\eta(x,t)$.

We introduce four terms from the geologic nomenclature that will facilitate later discussion. In the context of this development, regression and transgression refer, respectively, to the seaward ($\dot{s} > 0$) and landward ($\dot{s} < 0$) migration of the shoreline. Progradation and retrogradation refer, respectively, to the seaward growth ($\dot{u} > 0$) and landward retreat ($\dot{u} < 0$) of the entire fluvio-deltaic system; note that shoreline transgression is possible in a prograding fluvio-deltaic system.

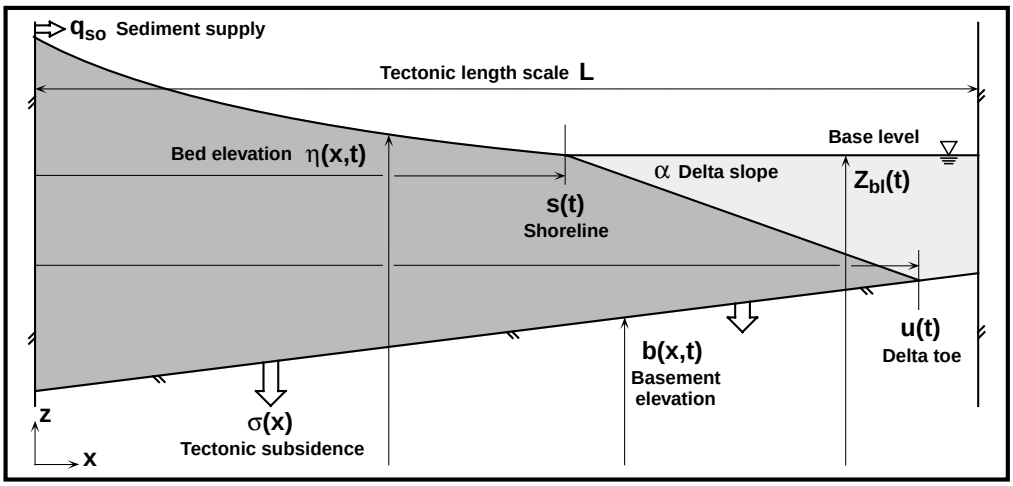

FIGURE 2. Cross section of an idealized basin used in the mathematical model.

Sediment transport in the submarine section, $s(t) \leqslant x \leqslant u(t)$, is dominated by avalanche processes. In our model, submarine slope readjustment proceeds at a rate that is large relative to that which characterizes fluvial sediment transport such that the delta maintains a linear profile of slope α, where in general α is a function of grain size, pore pressure, and seismicity. We ignore the net offshore transfer of sediment by wind- and tide-generated currents. Our model of passive (grain flow) submarine sediment transport is most applicable to coarse-grained systems with low wave energy, in which transport of sediment in suspension is minimal.

Sediment transport in the fluvial section is diffusional. The sediment flux, $q_s(x,t)$, varies linearly with the slope of the sediment-water interface such that the sediment continuity equation reduces to a linear diffusion equation in $\eta(x,t)$ with a sink term to represent sediment extraction via tectonic subsidence,

$$\frac{\partial \eta}{\partial t} + \sigma(x) = \upsilon \frac{\partial^2 \eta}{\partial x^2}, \qquad 0 \leqslant x \leqslant s(t), \tag{2.1}$$

where the sediment diffusivity, υ, depends primarily on the water discharge in the fluvial system [14]. The appendix contains a simplified derivation of (2.1).

We apply the following boundary conditions to (2.1)

$$\left.\frac{\partial \eta}{\partial x}\right|_{0,t} = -\frac{q_{so}}{\upsilon}, \tag{2.2}$$

$$\eta(s,t) = Z_{bl}(t). \tag{2.3}$$

The Neumann condition (2.2) relates the bed slope at the basin's upstream boundary to the strength of the sediment line source, and the Dirichlet condition (2.3) equates the bed elevation at the shoreline to base level. An additional relation is required to locate the shoreline and thereby close the problem. We enforce global sediment conservation

$$q_{so} = \frac{d}{dt}\int_0^s (\eta - b)dx + \frac{d}{dt}\int_s^u [Z_{bl} + \alpha(s-x) - b]dx, \tag{2.4}$$

https://doi.org/10.1017/S0956792500004198 Published online by Cambridge University Press

and use the relations

$$\frac{\partial b}{\partial t} = -\sigma(x), \qquad (\eta - b)|_{u,t} = 0, \tag{2.5}$$

to derive an expression for sediment transfer between the fluvial and deltaic regimes

$$-\upsilon \frac{\partial \eta}{\partial x}\bigg|_{s,t} = q_s(s,t) = (u-s)\left(\alpha \frac{ds}{dt} + \frac{dZ_{bl}}{dt}\right) + \int_s^u \sigma(x)dx. \tag{2.6}$$

Equation (2.6) can be derived from purely geometric arguments.

The incipient basin has no fluvial section, a uniform water depth of H, and an initial delta length of $H \cdot \alpha^{-1}$. The initial condition is

$$s(0) = 0. \tag{2.7}$$

Subsidence is the sum of constant and deviatoric terms, both of which scale with the mean subsidence rate

$$\sigma(x) = \overline{\sigma}\left[1 + \chi\Gamma\left(x \cdot L^{-1}\right)\right], \tag{2.8}$$

where Γ is a dimensionless, $O(1)$ function, and χ sets the amplitude of the deviatoric term. Note that the tectonic length scale (L) is embedded in Γ. We restrict our analysis to a continuum of first-order subsidence profiles, for which

$$\Gamma = -1 + 2x \cdot L^{-1}, \qquad \chi \in [-1, 1]. \tag{2.9}$$

Likewise, the base level is the sum of equilibrium and periodic components

$$Z_{bl}(t) = Z_{eq} + A\zeta\left(t \cdot T^{-1}\right), \tag{2.10}$$

where ζ is any dimensionless, periodic, $O(1)$ function. Here, we impose sinusoidal forcing,

$$\zeta(t) = \sin 2\pi t \cdot T^{-1} \tag{2.11}$$

and allow $Z_{eq} \to 0$. In the interest of generality, we retain the Γ and ζ notation.

We restrict our analysis to progradation ($\dot{u} > 0$) across basement, in which case the position of the delta toe is

$$u(t) = [A\zeta + \alpha s + H + (1-\chi)\overline{\sigma}t] \cdot \left(\alpha - 2\chi\frac{\overline{\sigma}t}{L}\right)^{-1}. \tag{2.12}$$

The seaward basin boundary is defined by a symmetry plane, parallel to the $y-z$ plane, at $x = L$. Should the delta toe intersect this plane, its position will remain fixed, i.e. $u = L$, though its elevation may vary according to the balance between sedimentation and subsidence rates. In general, if the rate of relative base-level rise, i.e. $\sigma + \dot{Z}_{bl}$, is sufficiently large, the delta toe may retreat, in which case the system is retrogradational, (2.12) no longer holds, and the position of the delta toe is determined via its intersection with previously deposited sediments. We do not address this scenario here, as the additional complexity would blur the analysis.

https://doi.org/10.1017/S0956792500004198 Published online by Cambridge University Press

3 A generalized Stefan problem

We can write (2.6) as an integro-differential equation for the shoreline trajectory

$$(u-s)\alpha\frac{ds}{dt} = q_s(s,t) - (u-s)\frac{dZ_{bl}}{dt} - \int_s^u \sigma(x)dx. \tag{3.1}$$

The fluvial system cannot extract sediment from the delta, i.e. $q_s(s,t) \geqslant 0$, which is equivalent to a statement of unidirectional mass transfer across the shoreline. The rate of shoreline translation is thus determined by the balance between sediment supplied to the shoreline by the fluvial system, $q_s(s,t)$, and the net rate at which space is created or destroyed across the delta by the combination of tectonic subsidence and fluctuations in base level. If this balance is positive, i.e. if the fluvial system can deliver more sediment to the shoreline than is required to maintain the present delta configuration, the shoreline will advance; conversely, if this balance is negative, the shoreline will retreat such that the fluvial system is shortened sufficiently for (3.1) to be satisfied with $q_s(s,t) \geqslant 0$.

Our model of fluvio-deltaic sedimentation is a generalized Stefan problem [3], in which the shoreline is analogous to a melting front, the fluvial bed elevation is equivalent to the temperature distribution in a conduction-dominated liquid phase, base level and water depth at the delta toe are analogous to the time-dependent melting temperature and latent heat, respectively, and tectonic subsidence can be envisaged as a distributed heat sink in the liquid phase. We interpret (3.1) as a generalized Stefan condition that equates the rate of shoreline translation to the sum of sediment flux delivered to the shoreline by the fluvial system and a pair of source/sink terms that embodies the net rate at which space is created across the delta.

In the limit of zero subsidence ($\overline{\sigma} \to 0$), steady base level ($\dot{Z}_{bl} \to 0$), and uniform water depth H, the governing equation (2.1), boundary conditions (2.2, 2.3, and 2.6), and initial condition (2.7) reduce to

$$\frac{\partial\eta}{\partial t} = \upsilon\frac{\partial^2\eta}{\partial x^2}, \qquad 0 \leqslant x \leqslant s(t), \tag{3.2}$$

$$\left.\frac{\partial\eta}{\partial x}\right|_{0,t} = -\frac{q_{so}}{\upsilon}, \tag{3.3}$$

$$\eta(s,t) = 0, \tag{3.4}$$

$$-\upsilon\left.\frac{\partial\eta}{\partial x}\right|_{s,t} = q_s(s,t) = H\frac{ds}{dt}, \tag{3.5}$$

$$s(0) = 0, \tag{3.6}$$

In this limit, the analogy to the fixed-flux, single-phase Stefan problem [3] is exact.

4 Dimensional analysis

In this section, we use the length, elevation, and time scales, L, $q_{so}L \cdot \upsilon^{-1}$, and $L^2 \cdot \upsilon^{-1}$, respectively, to recast the governing equations in dimensionless form and thereby identify a set of dimensionless groups that (1) controls the behaviour of a subsiding fluvio-deltaic basin with unsteady base level and (2) allows for the meaningful comparison of shoreline

https://doi.org/10.1017/S0956792500004198 Published online by Cambridge University Press

trajectories from basins of differing size, sediment supply, transport efficiency, and tectonic style. The basin of Figure 2 is described by a set of six independent, dimensionless groups

$$\{e_m, \Lambda, \chi, b_o, \epsilon, \tau\} \equiv \left\{ \frac{q_{so}}{\alpha \upsilon}, \frac{q_{so}}{\bar{\sigma} L}, \chi, \frac{H\upsilon}{q_{so} L}, \frac{A\upsilon}{q_{so} L}, \frac{T\upsilon}{L^2} \right\}, \tag{4.1}$$

which defines a parameter space for the problem.

If sediment transport in the marine regime is slope-dependent, then the ratio of slope scales, e_m, is the relative efficiency of marine sediment transport; we expect $e_m < 1$. The capture ratio, Λ, embodies the global balance between sediment supplied to the basin and the rate at which space is created by tectonic subsidence [13]. The basin's spatial distribution of subsidence, i.e. its tectonic style, is controlled by χ. The dimensionless initial water depth is b_o. Finally, ϵ and τ are the dimensionless amplitude and period of any imposed base-level forcing.

It is instructive to quantify the length, elevation, and time scales that characterize a subsiding fluvio-deltaic basin. We are interested in modelling the deposition of kilometers of sediment on geologic time scales, i.e. tens of million of years, in basins with tectonic length scales of hundreds of kilometers and for which sea level is base level. We define a representative basin with a tectonic length scale (L) of 10^3 km and a fluvial diffusivity (υ) of 10^6 m$^2 \cdot$ a^{-1}, which together yield a basin response time ($L^2 \cdot \upsilon^{-1}$) of one million years (1 Ma). (The Appendix contains a derivation of υ and the calculation of its value for this representative basin.) The fluvial slope scale for a basin of this size does not exceed a few parts in a thousand, and we set $q_{so} \cdot \upsilon^{-1} = 10^{-3}$ for the representative basin, which yields an elevation scale ($q_{so} L \cdot \upsilon^{-1}$) of 1 km.

The depositional slope scale of the marine system (α) is greater than that of its fluvial counterpart, and based on observation we do not expect the ratio of slopes scales, i.e. e_m, to be less than a few parts in a hundred [18]. Hence, $10^{-2} < e_m < 10^0$, and we assign the representative basin a marine efficiency of 10^{-1}. The choice of representative values for the remaining groups (Λ , χ , and b_o) is somewhat arbitrary. We restrict our analysis to starved basins, for which $0 < \Lambda < 1$, and set $\Lambda = 0.5$. The representative basin has no deviatoric subsidence component ($\chi = 0$). The only restriction on b_o is that the dimensionless initial delta length be small relative to unity; we assign b_o a value of 10^{-1}, which gives $u(0) = 10^{-2}$. The representative basin thus occupies the point $\{0.1, 0.5, 0.0, 0.1\}$ in the subspace $\{e_m, \Lambda, \chi, b_o\}$.

We can constrain the values of ϵ and τ by considering two widely accepted mechanisms for global (eustatic) sea-level change. First, variations in the rate of sea-floor spreading are thought to produce high-amplitude, low-frequency ($A \approx 10^2$ m, $10^1 < T < 10^2$ Ma) eustatic fluctuations [16]. Second, changes in the volume of continental ice sheets have been shown to generate high-amplitude, high-frequency ($10^1 < A < 10^2$ m, $10^{-2} < T < 10^0$ Ma) glacio-eustatic fluctuations [5]. Thus, for $q_{so} L \cdot \upsilon^{-1}$ and $L^2 \cdot \upsilon^{-1}$ of 1 km and 1 Ma, respectively, we might expect $0 < \epsilon < 10^{-1}$ and $10^{-2} < \tau < 10^2$. We define a representative base-level cycle by $\{\epsilon, \tau\} = \{5 \cdot 10^{-2}, 10^0\}$.

The dimensionless governing equation, boundary conditions, and initial condition are

$$\frac{\partial \eta}{\partial t} + \frac{1}{\Lambda} [1 + \chi \Gamma(x)] = \frac{\partial^2 \eta}{\partial x^2}, \qquad 0 \leqslant x \leqslant s(t), \tag{4.2}$$

https://doi.org/10.1017/S0956792500004198 Published online by Cambridge University Press

$$\left.\frac{\partial \eta}{\partial x}\right|_{0,t} = -1, \tag{4.3}$$

$$\eta(s,t) = \epsilon\zeta(t \cdot \tau^{-1}), \tag{4.4}$$

$$-\left.\frac{\partial \eta}{\partial x}\right|_{s,t} = q_s(s,t) = (u-s)\left(\frac{1}{e_m}\frac{ds}{dt} + \epsilon\frac{d\zeta}{dt} + \frac{1}{\Lambda}\right) + \frac{\chi}{\Lambda}\int_s^u \Gamma(x)dx, \tag{4.5}$$

$$s(0) = 0, \tag{4.6}$$

where for the remainder of the manuscript, unless otherwise noted, all variables are dimensionless. With Γ given by (2.9), the position of the delta toe is

$$u(t) = \left[\frac{s}{e_m} + \epsilon\zeta + b_o + \frac{t}{\Lambda}(1-\chi)\right] \cdot \left(\frac{1}{e_m} - 2t\frac{\chi}{\Lambda}\right)^{-1}. \tag{4.7}$$

Note that we recover the limiting case of § 3 with $\Lambda \to \infty$, $b_o \to 1$, $\epsilon \to 0$, and χ and τ irrelevant.

5 Solution techniques

5.1 Numerical method

A closed-form analytical solution to (4.2)–(4.7) is unavailable. We obtain a numerical solution via a front-tracking, control-volume approach, similar to that described in Voller and Peng [20], with 101 uniformly distributed nodes. To capture accurately the small-time shoreline behavior, we use a logarithmic temporal discretization. The fluvial bed elevation and the (non-zero) shoreline position at the initial simulation time are approximated with a semi-analytical solution discussed below.

5.2 Mass Balance Integral (MBI) method

Integral-profile methods commonly are used to obtain approximate, semi-analytical solutions to moving-boundary problems. The classic example is the Heat-Balance Integral approach used in solidification studies, whereby the temperature distribution is approximated with a low-order polynomial and the principle of global energy conservation used to derive an ordinary differential equation in the position of the phase front [6]. We use a modified version of this approach – the Mass Balance Integral (MBI) method – to generate approximate shoreline trajectories from (4.2)–(4.7).

The approximate fluvial bed elevation is the sum of a polynomial of order M and base level

$$\eta(x,t) \approx \sum_{m=1}^{M} a_m(s-x)^m + \epsilon\zeta, \qquad 0 \leqslant x \leqslant s(t). \tag{5.1}$$

For steady sediment supply, the global sediment budget is simply

$$\int_0^u (\eta - b) = t + \tfrac{1}{2}e_m b_o^2, \tag{5.2}$$

where the second term on the right-hand side of (5.2) is the area of the sediment wedge

https://doi.org/10.1017/S0956792500004198 Published online by Cambridge University Press

filling the incipient basin. Expanding (5.2) gives a polynomial of order $M+1$ in $s(t)$

$$\sum_{m=1}^{M} \frac{a_m}{m+1} s^{m+1} - \frac{1}{2e_m}(u-s)^2 + (b_o + \epsilon\zeta)u + \frac{ut}{\Lambda}\left[1 + \chi(u-1)\right] = t + \tfrac{1}{2}e_m b_o^2. \tag{5.3}$$

We limit the present analysis to $M \leqslant 3$, for which the a_m satisfy

$$a_1^2 + c_1 a_1 + c_0 = 0,$$

$$c_1 = (s-u)\left[\epsilon\frac{d\zeta}{dt} + \frac{1}{\Lambda} + \frac{\chi}{\Lambda}(u+s-1) - \frac{1}{e_m s}\left(\delta_{M,2} + \delta_{M,3}\right)\right], \tag{5.4}$$

$$c_0 = \frac{(u-s)}{e_m}\left[\epsilon\frac{d\zeta}{dt} + \frac{1}{\Lambda}(1-\chi+2\chi s) - \frac{1}{s}\delta_{M,2} - \left(\frac{1}{s} + \frac{\chi}{\Lambda}s\right)\delta_{M,3}\right],$$

$$a_2 = \frac{1}{2s}\left(1 - a_1 + \frac{\chi}{\Lambda}s^2\delta_{M,3}\right)\left(\delta_{M,2} + \delta_{M,3}\right), \tag{5.5}$$

$$a_3 = -\frac{\chi}{3\Lambda}\delta_{M,3}, \tag{5.6}$$

(δ is the Kroneker delta function.) We determine the a_m as follows:

(i) Equation (5.6) is a consequence of steady sediment supply

$$\left.\frac{dq_s}{dt}\right|_{0,t} = \left.\frac{\partial^3\eta}{\partial x^3}\right|_{0,t} - \left.\frac{\chi}{\Lambda}\frac{d\Gamma}{dx}\right|_0. \tag{5.7}$$

(ii) The Neumann condition at the sediment source gives (5.5).

(iii) We obtain (5.4) by enforcing the shoreline Stefan condition and then using the rate of change in bed elevation at the shoreline

$$\left.\frac{d\eta}{dt}\right|_{s,t} = \frac{ds}{dt}\cdot\left.\frac{\partial\eta}{\partial x}\right|_{s,t} + \left.\frac{\partial^2\eta}{\partial x^2}\right|_{s,t} - \frac{1}{\Lambda}\left[1 + \chi\Gamma(s)\right] = \epsilon\frac{d\zeta}{dt} \tag{5.8}$$

to eliminate the explicit dependence on $\dot{s}$, which reduces (5.3) to a simple transcendental equation in $s(t)$.

For the case of $M = 1$ an alternative approach is to satisfy the Neumann condition at the sediment source, in which case $a_1 = 1$. We demonstrate below that this approach often gives satisfactory results.

6 Results

In this section we present shoreline trajectories generated from numerical and semi-analytical solutions to the governing equations of § 4; due to space limitations, we present a single cross section of basin strata.

6.1 The representative basin's stratigraphic response with steady base level

The representative basin's strata and corresponding shoreline trajectory (numerical and semi-analytical solutions) are shown in Figures 3 and 4, respectively. The trajectory is

https://doi.org/10.1017/S0956792500004198 Published online by Cambridge University Press

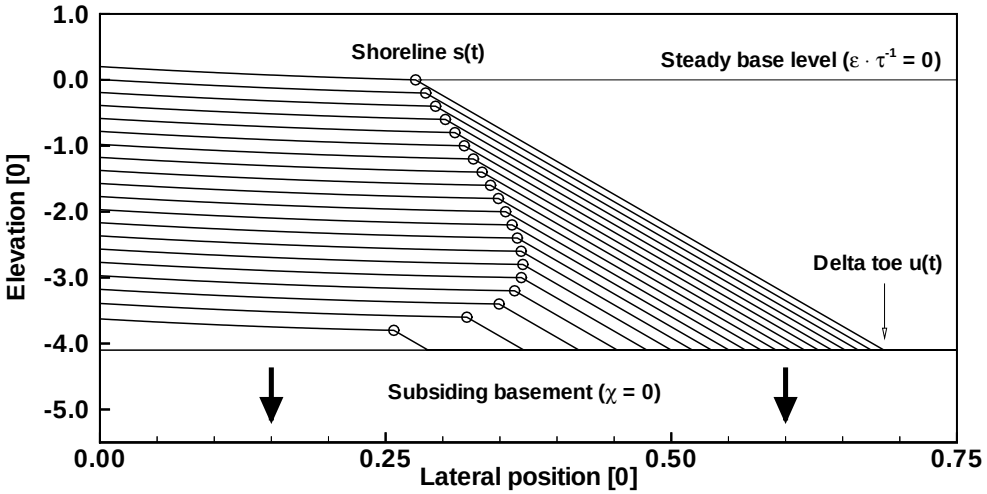

FIGURE 3. Representative basin's strata at $t = 2.0$ with temporal spacing of $\Delta t = 0.1$.

characteristic of a starved ($\Lambda < 1$) fluvio-deltaic basin with steady base level ($\epsilon \cdot \tau^{-1} = 0$) and displays a relatively brief period of regression ($\dot{s} > 0$) followed by an extended period of transgression ($\dot{s} < 0$), which culminates in the complete drowning of the basin ($s \to 0$). This prolonged period of shoreline retreat is a manifestation of the volumetric imbalance between the basin's sediment supply (q_{so}) and the rate at which subsidence creates space to be filled ($\overline{\sigma} L$). Muto & Steel [11] termed this phenomenon 'autoretreat,' and we will refer to a shoreline trajectory of the form shown in Figure 4 as an autoretreat trajectory.

With reference to Figure 4, we define several autoretreat parameters. We denote by T_{fluv}, s_{ar}, and t_{ar} the fluvial lifespan, i.e. the time interval over which the system maintains a fluvial component ($s > 0$), the shoreline maximum in the autoretreat trajectory, and the onset of autoretreat, respectively. In all subsiding fluvio-deltaic basins with $\epsilon \cdot \tau^{-1} = 0$, maximum regression ($\dot{s} = 0$) corresponds to the onset of autoretreat.

Historically, quantitative treatments of shoreline migration presume the existence of an equilibrium state in which the shoreline is stationary [16, 8]. Typically, this is realized by subjecting the basin to steady external forcing (sediment supply, subsidence, and base level) such that it evolves to a state in which the rates of sedimentation and subsidence are everywhere equal. Fluctuations in the basin's boundary conditions drive it from this equilibrium state. Hence, in the context of traditional models, a shoreline regression/transgression preserved in the rock record is attributed to a temporal variation in sediment supply, subsidence rate, base level, or some combination thereof. A direct consequence of our analysis is that, in general, the basin does not possess an equilibrium configuration, and the aforementioned regression/transgression might be a natural consequence of long-term sediment starvation rather than a change in basin boundary conditions. Our model admits a steady-state solution if $\Lambda = 1$, $\epsilon \cdot \tau^{-1} = 0$, and the movement of the delta toe is arrested by a discontinuity in subsidence at the distal boundary, i.e. by a cliff at $x = u = 1$.

https://doi.org/10.1017/S0956792500004198 Published online by Cambridge University Press

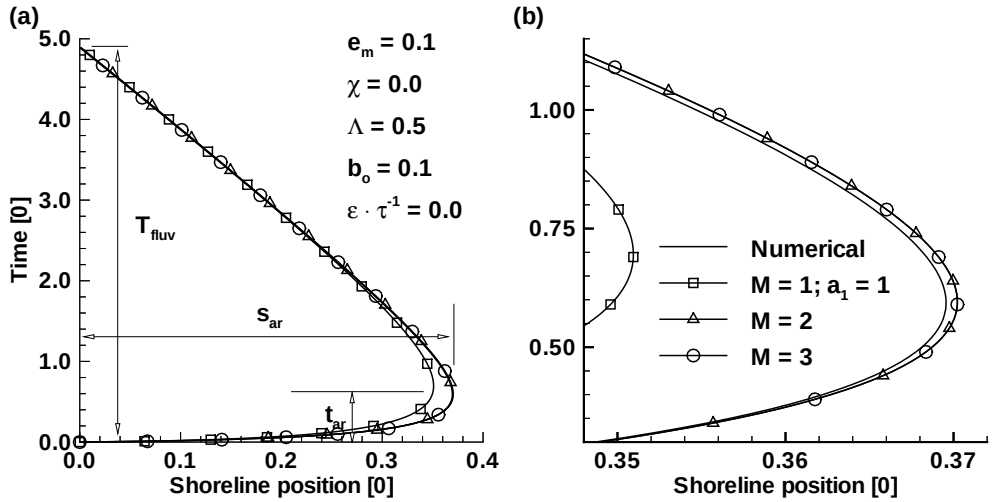

FIGURE 4. (a) The characteristic autoretreat shoreline trajectory of a subsiding fluvio-deltaic basin with steady base level. The solid curve is the numerical solution; open symbols denote the semi-analytical solution with polynomials of order M, $M = 1, 2$, and 3. (b) Exploded view of $s - t$ space near the onset of autoretreat.

6.2 Comparison of solution techniques

Before embarking on an exploration of the basin's parameter space, we compare the numerical and semi-analytical (MBI) solution techniques. In the interest of conserving space, we limit our discussion to the trajectories of Figure 4.

When viewed over the basin's fluvial lifespan, the numerical and nonlinear ($M = 2, 3$) MBI solutions are nearly degenerate (Figure 4(a)). Figure 4(b) shows the region of $s - t$ space near the onset of autoretreat where the difference in trajectories is greatest. The quadratic and cubic solutions are indistinguishable at this scale, and neither differs from the numerical solution by more than 0.2%. The linear solution ($M = 1$) with $a_1 = 1$ compares well with numerical and higher-order MBI solutions everywhere but near the onset of autoretreat, where it underestimates the shoreline position by no more than 5% relative to the numerical solution. Unfortunately, a linear trial function that satisfies the shoreline Stefan condition (4.5) admits a non-physical, complex shoreline trajectory. In general, the level of agreement between the numerical and nonlinear MBI solutions shown in Figure 4 persists throughout those regions of the full parameter space that we investigate below.

6.3 The shoreline response of a subsiding basin with steady base level

In this section, we explore systematically the subspace $\{e_m, \Lambda, \chi, b_o\}$ to determine the influence on shoreline trajectory (relative to that of the representative basin) of variations in each group. We accomplish this by varying each group over a geologically plausible range and constructing a corresponding suite of shoreline trajectories; in each suite, the solid curves and open symbols represent the numerical and MBI ($M = 3$) solutions, respectively.

https://doi.org/10.1017/S0956792500004198 Published online by Cambridge University Press

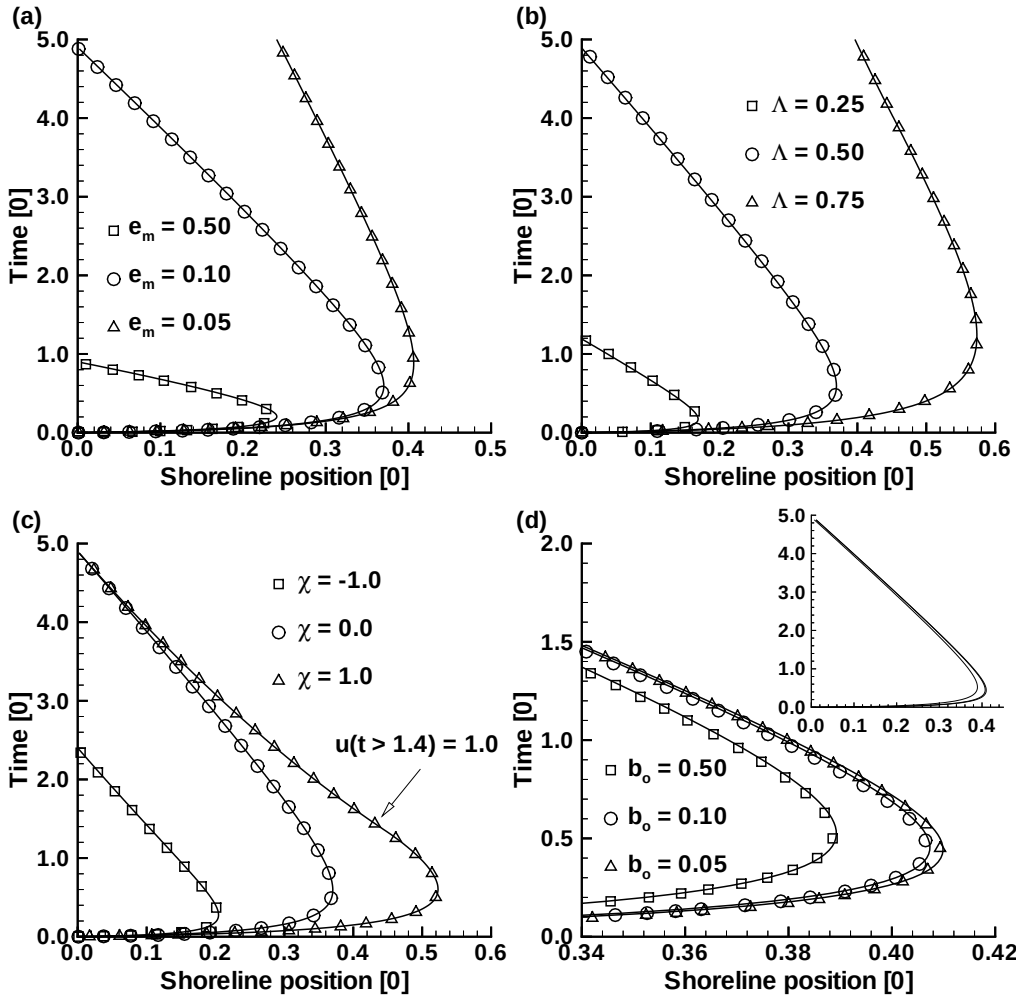

FIGURE 5. Sensitivity of the autoretreat shoreline trajectory to variations in (a) marine efficiency (e_m), (b) capture ratio (Λ), (c) tectonic style (χ), and (d) initial water depth (b_o). The solid curves and open circles denote the numerical and semi-analytical ($M = 3$) solutions, respectively.

We begin by investigating the effects of an order-of-magnitude variation in marine efficiency (Figure 5(a)). The fluvial lifespan is strongly dependent on the marine efficiency: a basin with $e_m \approx 1$ is characterized by $T_{fluv} \approx 1$, whereas a system with $e_m << 1$, which is more typical of real basins, is characterized by $T_{fluv} >> 1$. Apparently, inefficient marine transport prolongs the basin's lifespan. The explanation for this behavior is geometric. For a given water depth, as e_m increases, so does the delta length and, correspondingly, the shoreline sediment flux required to maintain progradation. The shoreline maximum and the onset of autoretreat display a weaker dependency on marine efficiency; as e_m increases both s_{ar} and t_{ar} decrease monotonically.

The influence of the capture ratio (Λ) on shoreline trajectory is shown in Figure 5(b). Recall that Λ^{-1} scales the strength of the sink term in (2.1). An emaciated basin ($\Lambda << 1$)

https://doi.org/10.1017/S0956792500004198 Published online by Cambridge University Press

suffers a limited fluvial lifespan ($T_{fluv} << 1$), an early onset of autoretreat ($t_{ar} << 1$), and a highly attenuated shoreline maximum ($s_{ar} << 1$). Conversely, a slightly starved basin ($\Lambda \approx 1$) enjoys a long fluvial lifespan ($T_{fluv} >> 1$), a delayed onset of autoretreat ($t_{ar} \approx 1$), and an $O(1)$ shoreline maximum ($s_{ar} \approx 0.5$).

The shoreline response to variations in tectonic style (χ) is shown in Figure 5(c). All three autoretreat parameters, T_{fluv}, t_{ar}, and s_{ar}, increase with increasing χ. We explain this behavior by noting that progradation in a basin with $\chi < 0$ occurs predominantly within a region ($x < 0.5$) where the rate of subsidence exceeds the mean value. The opposite is true of a basin characterized by $\chi > 0$. For $\chi = 1$, the reduced rate of autoretreat for $t > 1.4$ is a consequence of the delta toe intersecting the symmetry plane at $x = 1$, which reduces the rate of delta lengthening and, by sediment continuity, the rate of fluvial shortening.

Finally, in Figure 5(d) we show the effects of an order-of-magnitude variation in initial water depth, b_o, which affects primarily the initial rate of shoreline advance. The influence of b_o is most discernible near the onset of autoretreat, where it appears that a decrease in initial water depth yields a slight decrease in t_{ar} and a minor increase in s_{ar}. However, when viewed over the fluvial lifespan of the basin, the shoreline trajectories are nearly degenerate (Figure 5(d), inset). Our analysis indicates that variations in b_o have minimal impact on the autoretreat parameters, from which we conclude that a fluvio-deltaic basin is relatively insensitive to its initial configuration.

6.4 The effects of base-level cycling

In this section we demonstrate the sensitivity of the representative basin's shoreline trajectory to changes in base level. To illustrate this, we consider independently the shoreline response to variable-amplitude and variable-frequency sinusoidal base-level cycling. Throughout this exercise, the remaining controlling groups are fixed at their representative values given in § 4.

In Figure 6 we show the shoreline trajectory generated with a representative base-level cycle, i.e. $\{\epsilon, \tau\} = \{5 \cdot 10^{-2}, 10^{0}\}$, together with its corresponding autoretreat ($\epsilon \cdot \tau^{-1} = 0$) trajectory of Figure 4. The figure focuses on the region of $s - t$ space near the onset of autoretreat, where the effects of base-level forcing are most pronounced. During periods of sub-equilibrium ($\zeta < 0$) and super-equilibrium ($\zeta > 0$) base level, the shoreline trajectory generally is situated outboard (seaward) and inboard (landward), respectively, of the autoretreat trajectory. To first order, the shoreline response is in phase with base level such that maxima and minima in shoreline position correspond approximately to minima and maxima in base level, respectively. The amplitude of shoreline response is, however, a function of the basin's age; the basin progressively attenuates the base-level signal with increasing age.

We treat the shoreline response to base-level cycling as the superposition of base-level and autoretreat trajectories and define a residual shoreline, s_{res}, as the difference between the shoreline response to base-level forcing and the corresponding autoretreat trajectory, s_{auto}, for which $\epsilon \cdot \tau^{-1} = 0$:

$$s_{res}(t) = s(t) - s_{auto}(t). \tag{6.1}$$

If the basin remains progradational throughout base-level cycling, i.e. if $\epsilon \cdot \tau^{-1} << 1$, then

https://doi.org/10.1017/S0956792500004198 Published online by Cambridge University Press

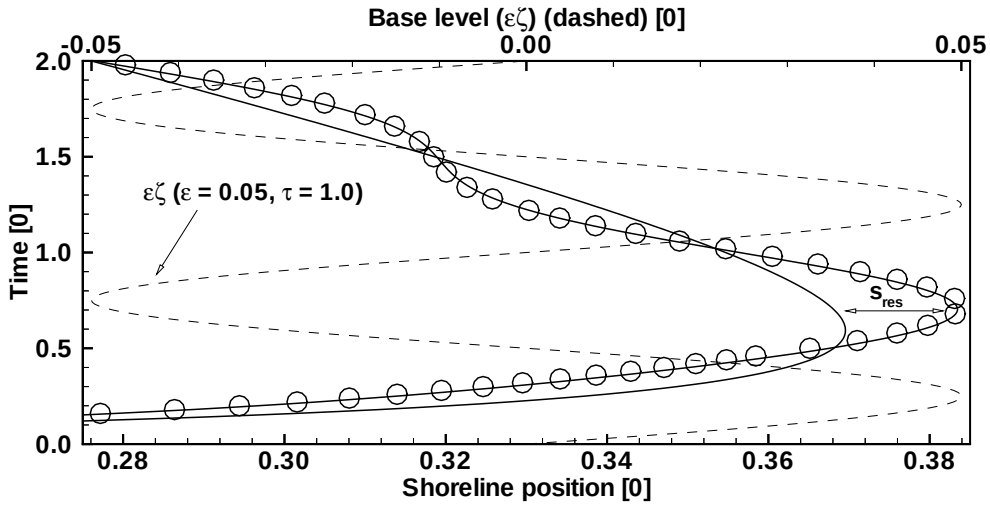

FIGURE 6. The shoreline response of the representative basin to representative base-level cycling. The solid curve and open symbols denote the numerical and semi-analytical ($M = 3$) solutions, respectively. The bold curve is the autoretreat trajectory of Figure 4. The dashed curve is base level ($\epsilon\zeta$).

to first order the residual shoreline response is

$$s_{res}(t) \approx -\epsilon \cdot f_t \cdot \zeta \left(t \cdot \tau^{-1} + \varphi\right). \tag{6.2}$$

The amplitude of the shoreline response scales (geometrically) with ϵ. The transfer function, f_t, embodies the basin's capacity to amplify/attenuate the base-level signal relative to the geometric shoreline response ($f_t \to 1$). The phase shift between shoreline and base level is φ. In general, for a given point in the subspace $\{e_m, \Lambda, \chi, b_o\}$, both f_t and φ are functions of ϵ, τ, and t. By analysing the shoreline response to a range of amplitudes and frequencies, we can describe qualitatively the structure of f_t and φ.

Figure 7 shows the residual shoreline trajectories (numerical solutions only) generated by an order-of-magnitude variation in the amplitude of base-level forcing (with $\tau = 1$). Not unexpectedly, for $\epsilon << 1$, the transfer function is nearly independent of ϵ. The weak dependence of f_t on ϵ is asymmetric with respect to the sign of ζ. The basin appears to filter weakly high-amplitude forcing during super-equilibrium base level ($\zeta > 0$) and, conversely, filter weakly low-amplitude forcing during sub-equilibrium base level ($\zeta < 0$). The residual shoreline trajectory is approximately in phase with base level, i.e. $\varphi \approx 0$, regardless of the forcing amplitude.

The most striking feature of Figure 7 is the transfer function's strong dependence on basin age, which is a direct consequence of sediment starvation (autoretreat) and has a simple geometric explanation. If the fluvial slope at the shoreline changes with time, as it must by (4.5), then the amplitude of shoreline response to base-level cycling must change as well. In particular, during autoretreat ($t > t_{ar}$), the fluvial system shortens continually ($\dot{s} < 0$) while the delta lengthens continually ($\dot{u} > 0$). Therefore, the sediment flux and the fluvial slope at the shoreline increase with time, from which it follows (geometrically) that the amplitude of shoreline response must decrease with time.

https://doi.org/10.1017/S0956792500004198 Published online by Cambridge University Press

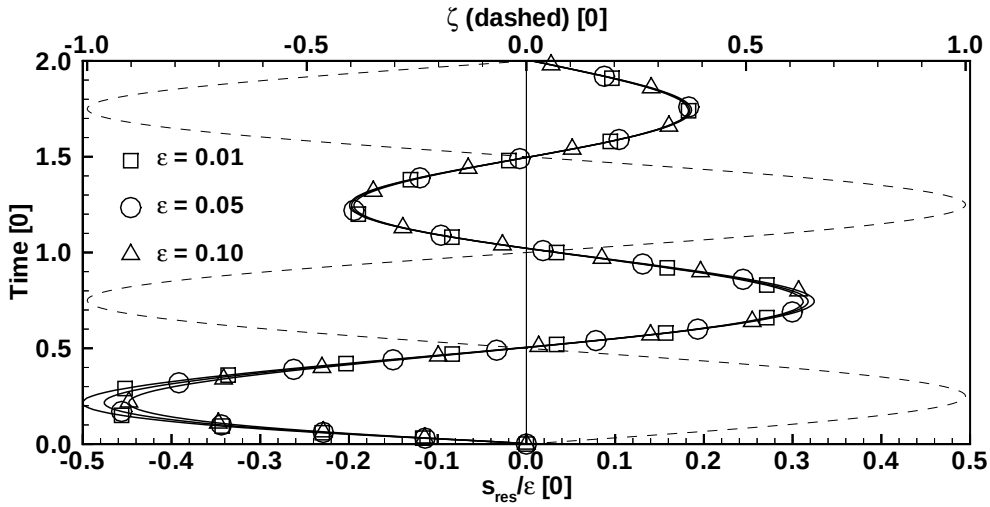

FIGURE 7. The residual shoreline responses (numerical solutions only; scaled with ϵ) to variable-amplitude base-level cycling with $\tau = 1$. The dashed curve is ζ.

In Figure 8 we show the residual shoreline trajectories generated by base-level cycling with a fixed amplitude of $\epsilon = 5 \cdot 10^{-2}$ and a period that varies according to 2^k, where $k = -1, 0, 1, 2$. Smaller values of k drive the basin into a retrogradational state, which we wish to avoid, and larger values of k yield $\tau > T_{fluv}$. The shoreline response to base-level cycling appears progressively attenuated with increasing τ, which would suggest that f_t is strongly dependent on τ; however, we believe that f_t is only weakly dependent on τ and that, instead, the attenuation is a consequence of the transfer function's dependence on basin age, as discussed above. To first order, s_{res} and ζ are in phase, i.e. $\varphi \approx 0$, regardless of the forcing frequency. However, there exists a weak, asymmetric phase shift that increases with decreasing forcing frequency and is most visible in the trajectories of Figure 8(b), for which $\tau = 2$ and $\tau = 4$. The shoreline response leads base level during super-equilibrium forcing, but is retarded during sub-equilibrium forcing such that $\varphi \approx 0$ over the entire cycle. At higher forcing frequencies ($\tau < 1$), the phase shift is very small ($\varphi << 1$), nearly symmetric over the cycle, and attenuated with increasing basin age (Figure 8(a)).

If a cycle of shoreline migration preserved in a basin's strata can be attributed unequivocally to a change in base level, then the first-order predictions of our analysis have important implications for solving the inverse problem. Our theory suggests that the amplitude of the driving base-level cycle is the product of the observed amplitude of shoreline migration (Δs; dimensioned), the fluvial slope scale ($q_{so} \cdot \upsilon^{-1}$), and the inverse of the $O(1)$ transfer function (f_t^{-1}). For a given amplitude of shoreline response, the amplitude of the driving base-level cycle increases with the basin's age; this manifestation of basin-scale sediment starvation is not captured in analyses that presume the existence of an equilibrium basin configuration. Furthermore, the amplitude of the driving base-level signal is largely independent of the time interval (T) represented by the shoreline cycle. To first order, times of maximum shoreline transgression and regression preserved in the strata correspond to maxima and minima in the driving base-level cycle. The last two predictions stand in contrast to those of previous analyses, which indicate that (1)

https://doi.org/10.1017/S0956792500004198 Published online by Cambridge University Press

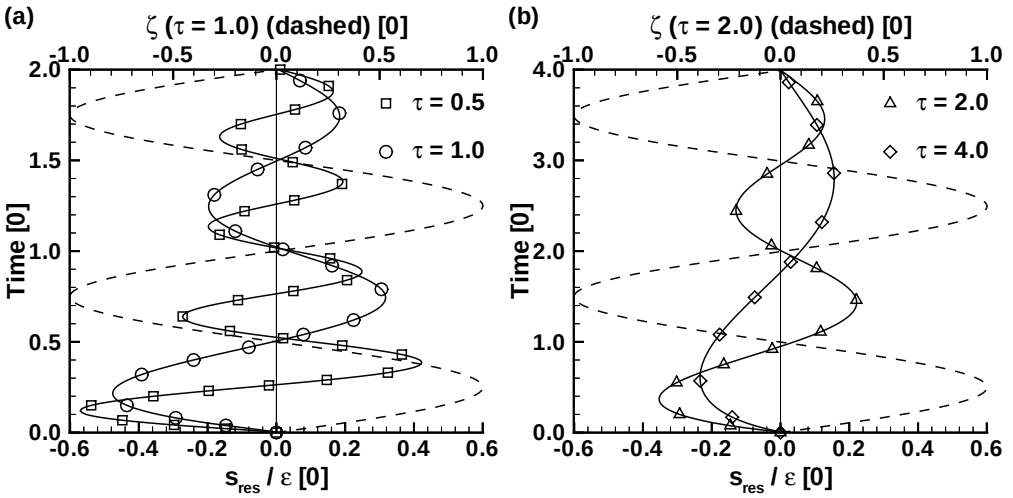

FIGURE 8. The residual shoreline responses (numerical solutions only; scaled with ϵ) to variable-frequency base-level cycling with $\epsilon = 5 \cdot 10^{-2}$. (a) $\tau = 2^{-1}, \tau = 2^{0}$; (b) $\tau = 2^{1}, \tau = 2^{2}$. The dashed curves represent ζ with $\tau = 2^{0}$ (a) and $\tau = 2^{2}$ (b).

the amplitude of the driving base-level cycle increases non-linearly with the duration of the preserved shoreline cycle and (2) times of maximum transgression and regression are potentially phase-shifted significantly ($\varphi \to 0.25$ for $\tau >> 1$) with respect to maxima and minima in base level [16, 2, 8].

7 Conclusions

We have presented an analysis of sedimentation in a subsiding fluvio-deltaic basin with steady sediment supply and unsteady base level and demonstrated that mass transfer in this system is analogous to heat transfer in a generalized Stefan problem. This observation allowed us to use generalizations of numerical and analytical solution techniques from the phase-change literature to generate shoreline trajectories. The salient points of our analysis are:

7.1 General shoreline behavior

(i) A subsiding basin with $\Lambda < 1$ and steady base level possesses a characteristic autoretreat [11] shoreline trajectory in which a brief period of regression is followed by an extended period of transgression, independent of the basin's location in the subspace $\{e_m, \Lambda, \chi, b_o\}$.

(ii) The autoretreat parameters, T_{fluv}, s_{ar}, and t_{ar}, increase with increasing Λ and χ and decreasing e_m.

(iii) The shoreline response is insensitive to the basin's initial bathymetry (b_o).

https://doi.org/10.1017/S0956792500004198 Published online by Cambridge University Press

7.2 The effects of base-level cycling

(i) The shoreline response to base-level cycling displays neither strong, frequency-dependent phase-shifting nor attenuation. This finding contradicts those of some earlier studies [16, 2, 8] and has important implications for the interpretation of the rock record (the inverse problem).

(ii) The amplitude of the shoreline response to base-level cycling in a starved ($\Lambda < 1$) basin is attenuated progressively with increasing basin age.

In summary, we note the following: (1) the present theory is testable, particularly the limiting case of § 3, which could be simulated in a standard flume; (2) a more complicated treatment of submarine sedimentation will alter but not destroy the analogy between mass transfer in a fluvio-deltaic system and heat transfer in a generalized Stefan problem; and (3) the dimensionless groups that appear in our governing equations are largely model-independent and characterize any subsiding fluvio-deltaic basin with slope-dependent sediment transport and periodic base level. Our analysis should thus serve as a point of departure for more complicated models of basin-scale sedimentation as a moving-boundary problem.

Acknowledgements

We thank Mark Person for generous access to the Gibson Computational Hydrogeology Laboratory at the University of Minnesota. This research was funded in part by National Science Foundation Grants GER-93-54936 and EAR-94-05807 (JBS), Minnesota Supercomputer Institute Grant (VRV), and a Schlumberger Foundation Grant (VRV).

Appendix A Diffusional fluvial sediment transport

The following derivation parallels that of Paola *et al.* [14]. Consider a unit width of basin normal to the mean transport direction, i.e. into the page in Figure 2, with a channelized fraction β and bed slope S. The flow is described by an average depth (h), velocity (U), and kinematic bed shear stress (τ_o), which is the shear stress divided by fluid density. Conservation of sediment volume in a subsiding, non-compacting basin is

$$(1-\phi_o)\left[\frac{\partial \eta}{\partial t}+\sigma(x)\right]=-\frac{\partial}{\partial x}(\beta q_s), \tag{A 1}$$

where ϕ_o is the depositional porosity ($\phi_o \approx 0.5$). Conservation of water volume is $q_w = \beta h U$, where q_w is normalized water discharge. Let h_o and S_o scale the flow depth and bed slope, respectively, within a channel. For length and time scales greater than $7h_o \cdot S_o^{-1}$ and $2h_o^2 \cdot (q_{so}S_o)^{-1}$, respectively, Ribberink & Van der Sande [19] showed that nonlinear ('backwater') terms are insignificant and the streamwise momentum balance simplifies to the depth–slope product, i.e. $\tau_o = ghS$, where g is gravitational acceleration. We relate τ_o to the velocity through a dimensionless drag coefficient, i.e. $\tau_o = C_f U^2$, where $C_f \approx 10^{-2}$. Combining this relation, the depth-slope product, and continuity in water discharge, we find

$$\tau_o^{3/2} = -\beta^{-1} g q_w \sqrt{C_f} S, \tag{A 2}$$

https://doi.org/10.1017/S0956792500004198 Published online by Cambridge University Press

The semi-empirical relation of Meyer-Peter & Müller [12] provides a statement of momentum conservation for the transported sediment

$$q_s = \frac{8\,(\tau_o - \tau_{oc})^{3/2}}{g\,(s_g - 1)}, \tag{A 3}$$

where τ_{oc} is the critical kinematic shear stress required to initiate sediment motion on the bed and s_g is the sediment specific gravity ($s_g \approx 2.65$). In braided, gravel bed rivers with easily eroded banks, Parker [15] showed that $\tau_o \approx (1+\gamma)\,\tau_{oc}$, where $\gamma \approx 0.2 - 0.4$; conversely, in meandering, sand bed rivers with strong banks, $\tau_o >> \tau_{oc}$. To first order (A.3) reduces to a linear relationship between sediment flux and bed slope

$$\beta q_s = -q_w \frac{8\kappa\sqrt{C_f}}{g\,(s_g - 1)} \frac{\partial \eta}{\partial x}, \tag{A 4}$$

where, in a broad sense, κ is a function of channel type

$$\kappa = \begin{cases} \left[\gamma/(1+\gamma)\right]^{3/2}, & \text{braided} \\ 1, & \text{meandering.} \end{cases} \tag{A 5}$$

If we treat q_w and κ as constants within the basin's fluvial regime, then (A1) is a linear diffusion equation in η

$$\frac{\partial \eta}{\partial t} + \sigma(x) = \upsilon \frac{\partial^2 \eta}{\partial x^2}, \tag{A 6}$$

where the fluvial diffusivity depends primarily on the water discharge in the system,

$$\upsilon = q_w \frac{8\kappa\sqrt{C_f}}{(1-\phi_o)\,(s_g - 1)}. \tag{A 7}$$

With the above values of ϕ_o, C_f, and s_g, we find $\upsilon \approx q_w \kappa$.

In § 6, we assigned a representative basin a tectonic length scale of 10^3 km. The normalized water discharge (q_w) is the product of a catchment length, L_c, which often scales like L, and a precipitation rate, $\dot{p}$. With $L_c = L$, $\dot{p} = 1\ \mathrm{m \cdot a^{-1}}$ (a typical value for a humid climate), and $\kappa = 1$, we find $\upsilon \approx L$, or, for the representative basin, $\upsilon \approx 10^6\ \mathrm{m^2 \cdot a^{-1}}$.

References

[1] Allen, P. A. & Allen, J. R. (1990) *Basin Analysis*. Blackwell Scientific.

[2] Angevine, C. L. (1989) Relationship of eustatic oscillations to regressions and transgressions on passive continental margins. In: R. A. Price (ed.), *Origin and Evolution of Sedimentary Basins and Their Energy and Mineral Resources*, pp. 29–35. AGU, Washington, DC.

[3] Crank, J. (1984) *Free and Moving Boundary Problems*. Cambridge University Press.

[4] Flemings, P. B. & Jordan, T. E. (1989) A synthetic stratigraphic model of foreland basin development. *J. Geophys. Res.* **94**, 3851–3866.

[5] Gallup, C. D., Edwards, R. L. & Johnson, R. G. (1994) The timing of high sea levels over the past 200,000 years. *Science* **263**, 796–800.

[6] Goodman, H. R. (1958) The heat balance integral and its application to problems involving a change of phase. *Trans. ASME* **80**, 335–342.

[7] Jervey, M. T. (1988) Quantitative geologic modeling of siliciclastic rock sequences. In: C. K. Wilgus *et al.* (eds.), *Sea-Level Changes – An Integrated Approach*, *SEPM Spec. Pub.* **42**, 47–69.

[8] Jordan, T. E. & Flemings, P. B. (1991) Large-scale stratigraphic architecture, eustatic variation, and unsteady tectonism: a theoretical evaluation. *J. Geophys. Res.* **96**, 6681–6699.
[9] Kaufman, P., Grotzinger, J. P. & McCormick, D. S. (1991) Depth-dependent diffusion algorithm for simulation of sedimentation in shallow marine depositional systems. In: E. K. Franseen *et al.* (eds.), *Sedimentary Modeling: Computer simulations and methods for improved parameter definition*, *Kansas Geol. Survey Bull.* **233**, 489–508.
[10] Kenyon, P. M. & Turcotte, D. L. (1985) Morphology of a delta prograding by bulk sediment transport. *Geol. Soc. Am. Bull.* **96**, 1457–1465.
[11] Muto, T. & Steel, R. J. (1997) Principles of regression and transgression: The nature of the interplay between accommodation and sediment supply. *J. Sed. Res.* **67**, 994–1000.
[12] Meyer-Peter, E. & Müller, R. (1948) Formulas for bed-load transport. $2^{\underline{nd}}$ *Mtg Ing. Ass. Hyd. Structures Res.*, pp. 39–64.
[13] Paola, C. (1988) Subsidence and gravel transport in alluvial basins. In: K. L. Kleinsphen and C. Paola (eds.), *New Perspectives in Basin Analysis*, pp. 231–243. Springer-Verlag.
[14] Paola, C., Heller, P. L. & Angevine, C. L. (1992) The large-scale dynamics of grain-size variations in alluvial basins. *Basin Res.* **4**, 73–90.
[15] Parker, G. (1978) Self-formed straight rivers with equilibrium banks and mobile bed. Part 2. The gravel river. *J. Fluid Mech.* **89**, 127–146.
[16] Pitman, W. C. (1978) Relationship between eustacy and stratigraphic sequences on passive margins. *Geol. Soc. Am. Bull.* **89**, 1389–1403.
[17] Posamentier, H. W. & Vail, P. R. (1988) Eustatic controls on clastic deposition, II, Sequence and systems tract models. In: C. K. Wilgus *et al.* (eds.), *Sea-Level Changes – An Integrated Approach*, *SEPM Spec. Pub.* **42**, 125–154.
[18] Pratson, L. F. & Haxby, W. F. (1996) What is the slope of the U.S. continental slope? *Geology* **24**, 3–6.
[19] Ribberink, J. S. & Van der Sande, J. T. M. (1985) Aggradation in rivers due to overloading – analytical approaches. *J. Hyd. Res.* **23**, 273–284.
[20] Voller, V. R. & Peng, S. (1994) An enthalpy formulation based on an arbitrarily deforming mesh for solution of the Stefan problem. *Comp. Mech.* **14**, 492–502.